Structural Analysis of Apolipoprotein A-I: Effects of Amino- and Carboxy-Terminal Deletions on the Lipid-Free Structure†

Danise P. Rogers,‡ Linda M. Roberts,§ Jacob Lebowitz,|| Jeffrey A. Engler,*,‡ and Christie G. Brouillette*,‡,⊥

Department of Biochemistry and Molecular Genetics, Center for Macromolecular Crystallography, and Department of Microbiology, University of Alabama at Birmingham Medical Center, Birmingham, Alabama 35294, and Department of Chemistry, California State University at Sacramento, Sacramento, California 95819

Received June 6, 1997; Revised Manuscript Received October 15, 1997⊗

ABSTRACT: An amino-terminal deletion mutant (residues 1−43) and a carboxy-terminal deletion mutant (residues 187−243) of human apolipoprotein A-I (apo hA-I) have been produced from a bacterial expression system to explore the importance of the missing residues for the conformation of apo hA-I. Our focus has been to study the lipid-free structure of apo hA-I to understand how discrete domains influence the conformational plasticity of the protein and, by inference, the mechanism of lipid binding. All spectral and physical measurements indicate that both apo Δ(1−43)A-I and apo Δ(187−243)A-I have folded, tertiary structures. These structures differ in the specific arrangement of helical domains based, in part, on their relative thermodynamic stability, near- and far-UV CD, limited proteolysis, and the accessibility of tryptophans to fluorescence quenchers. In addition, all data indicate that the folded domains of apo hA-I and apo Δ(187−243)A-I are very similar. Results from analytical ultracentrifugation suggest that lipid-free apo hA-I and the deletion mutants each exist in a dynamic equilibrium between a loosely folded, helical bundle and an elongated monomeric helical hairpin. The conformational heterogeneity is consistent with significant ANS binding exhibited by all three proteins and could help to explain the facile lipid binding properties of apo hA-I.

Human apolipoprotein A-I (apo hA-I), a polypeptide of 243 amino acid residues, is the major structural protein of plasma high-density lipoproteins (HDL), comprising 70% of the total HDL protein. Apo hA-I is thought to mediate a variety of functions associated with HDL particles. In complexes with HDL, apo hA-I acts as the most potent physiological activator of the plasma enzyme lecithin: cholesterol acyltransferase (LCAT) (Fielding et al., 1972). In addition, apo hA-I binds and transports plasma lipid and increases cholesterol efflux from peripheral tissues in a process termed "reverse cholesterol transport" (Glomset, 1968; Fielding & Fielding, 1995). The concentration of plasma HDL is inversely correlated to the risk of developing coronary artery disease (CAD), and various studies have shown that apo hA-I is responsible for this protective effect (Schultz et al., 1993; Warden et al., 1993). Apo hA-I has been reported to be an important ligand in the binding of HDL to cellular membranes (Oram, 1986; Sviridov et al., 1996), and an apo hA-I-specific receptor has been identified in liver and nonplacental steroidogenic tissues (Acton et al., 1996; Wang et al., 1996), suggesting receptor-mediation in apo hA-I's role in reverse cholesterol transport.

Although the primary structures of all the major human apolipoproteins are known and many investigators have characterized the secondary structure of apo hA-I (Nolte & Atkinson, 1992; Segrest et al., 1990, 1992), there is little direct information regarding the tertiary structure of these proteins. Negative stain electron microscopy, X-ray scattering, and attenuated total reflection infrared spectroscopy have given low-resolution structural information on lipid-bound apo hA-I (Atkinson et al., 1976, 1980; Brasseur et al., 1990; Forte et al., 1971; Wald et al., 1990), and these results have been used in conjunction with the secondary structure predictions to propose structural models. While there is no crystal structure of apo hA-I, we have recently solved the crystal structure of the putative lipid-bound conformation of apo Δ(1−43)A-I (Borhani et al., 1997), which has provided considerable insight into the lipid-bound structure for apo hA-I. Two other apolipoprotein crystal structures have also been reported: the 22 kDa N-terminal receptor-binding fragment of human apo E (Wilson et al., 1991) and apolipophorin III from locust (Briter et al., 1991). Both structures are for the lipid-free states which contain helical bundles and might suggest a motif that could be

† Initial construction of these mutants was supported by Grant HL34343 from the National Institutes of Health. Subsequent analytical studies were supported by funds from the State of Alabama. Synthesis of oligonucleotides for site-directed mutagenesis and DNA sequencing was supported in part by NCI Grant P50 CA13148 to the UAB Comprehensive Cancer Center. Use of computer programs used for analysis of DNA sequences (from the Genetics Computer Group, Madison, WI) was supported in part by NIAID Grant P50 AI27767.

* To whom correspondence should be addressed.

‡ Department of Biochemistry and Molecular Genetics, University of Alabama at Birmingham Medical Center.

§ California State University at Sacramento.

|| Department of Microbiology, University of Alabama at Birmingham Medical Center.

⊥ Center for Macromolecular Crystallography, University of Alabama at Birmingham Medical Center.

⊗ Abstract published in *Advance ACS Abstracts,* December 15, 1997.

S0006-2960(97)01351-2 CCC: $15.00
Published on Web 01/03/1998

typical for the water-soluble conformation(s) of other apolipoproteins, e.g., apo hA-I (Brown et al., 1994; Roberts et al., 1997).

The exchangeable apolipoproteins exhibit different structures in the lipid-free versus the lipid-bound states. The conformational transition between the states and their modulation is likely to play a significant role in the process of lipoprotein formation, metabolism, and function. Recently, Gursky and Atkinson (1996) suggested that apo hA-I might represent another class of proteins whose main physiological function (e.g., binding lipid) is mediated via a molten globular apolipoprotein state in the plasma. Binding of apo hA-I to lipid induces an increase in α-helical content and enhances protein stability, probably through hydrophobic interactions between the nonpolar surfaces of the amphipathic helices and the lipid matrix. Recent structural studies using deletion mutants of apo hA-I suggested that the N-terminal 43 residues play an essential role in maintaining the lipid-free conformation in plasma (Rogers et al., 1997), while the C-terminal 48 residues, residues 193 through 243, are actively involved in protein−lipid interactions and may be the first domain to bind to lipid (Gursky & Atkinson, 1996; Ji & Jonas, 1995; Roberts et al., 1997; Schmidt et al., 1995).

A knowledge of the tertiary structure of lipid-free apo hA-I would be useful to our understanding of the mechanism by which apo hA-I binds to lipid. The focus of this paper is to describe structural studies on N-terminal and C-terminal deletion mutants, apo Δ(1−43)A-I and apo Δ(187−243) A-I, respectively, and apo hA-I, using a variety of physical and biochemical techniques that provide information on conformational heterogeneity as well as stability, such as sedimentation velocity experiments, ANS binding, denaturant-induced unfolding, near- and far-UV CD, fluorescence quenching, and limited proteolysis. Based on these data, we present a model for the lipid-free conformation of wild-type apo hA-I and propose a potential mechanism by which this molecule binds to lipid.

EXPERIMENTAL PROCEDURES

Preparation of Human Apo A-I. Human apo A-I (apo hA-I) in the methionine reduced state (Anantharamaiah et al., 1988) was purified by the method of Hughes et al. (1988). The purified protein was lyophilized and stored at −20 °C. The lyophilized protein was solubilized in 6 M guanidine hydrochloride in PBS (0.02 M phosphate, 0.15 M NaCl, 0.02% NaN_3, 1 mM EDTA, pH 7.4) and dialyzed against PBS containing 10 μM D,L-α-tocopherol, 50 μM ascorbic acid, and 1 mM EDTA for use in the experiments described. An extinction coefficient of 1.13 mL/(mg·cm) at 280 nm was used to determine apo hA-I concentration in 6 M guanidine hydrochloride (Pownall & Massey, 1986).

Construction and Expression of Apo Δ(1−43)A-I and Apo Δ(187−243)A-I. PCR amplification was used to construct a gene encoding the mature apo hA-I (243 residues), using the full-length cDNA (Cheung & Chan, 1983) as a template (Rogers et al., 1997). Single-stranded DNA from this plasmid was prepared by standard methods (Viera & Messing, 1987) and used for site-directed mutagenesis (Zoller & Smith, 1983), using the oligonucleotides (A) 5′-GGAGATATACAT**ATG***CATCACCATCACCATCAC*ATCGAAGGTCGTCACGAGCCACCGCAG-3′ (sense strand) and (B) 5′-GGAGAACGGCGGCTAAGCTTGAGTATTC-3′ (sense strand). Oligonucleotide (A) added a 6X-histidine tag (indicated by +his; nucleotides encoding the histidine tag are in italics; the N-terminal methionine is underlined and boldface type) and a Factor Xa cleavage site to the amino-terminal region of apo hA-I, and oligonucleotide (B) deleted the nucleotides encoding amino acids 187−243. Mutants were identified by colony hybridization using the mutagenic oligo(s) as a probe, and their identity was confirmed by double-stranded dideoxynucleotide DNA sequencing according to the manufacturer's instructions (Sequenase v.2.0; United States Biochemical, Cleveland, OH). The mutant gene product, apo Δ(187−243)A-I+his, was expressed in *E. coli* BL21(DE3) cells (Studier & Moffat, 1986) by growth of the transformed bacteria in sterile DYT media (10 g of casein peptone, 10 g of yeast extract, 5 g of NaCl, and 2 pellets of NaOH per liter) with 100 μg/mL ampicillin to an $OD_{600} = 0.9-1.0$. Expression of the chromosomal copy of the bacteriophage T7 RNA polymerase gene was then induced with 1 mM IPTG. After 4 h, the cells were harvested by centrifugation and resuspended in sterile PBS containing 10 μM D,L-α-tocopherol, 50 μM ascorbic acid (no EDTA or NaN_3).

The vector encoding apo Δ(1−43)A-I was constructed and the gene product expressed as described previously (Rogers et al., 1997).

Purification and Characterization of Apo Δ(1−43)A-I and Apo Δ(187−243)A-I. The resuspended *E. coli* cells containing the recombinant apo Δ(187−243)A-I+his were lysed by French press. Solid guanidine hydrochloride was added to the supernatant to a final concentration of 3 M, and the pH was adjusted to 7.7 using 0.3 M sodium phosphate. Nickel-conjugated agarose beads (Ni-NTA; QIAGEN, Chatsworth, CA) were washed with 3 M guanidine hydrochloride in 0.1 M sodium phosphate, pH 8.0, and then combined with the bacterial supernatant. The pH was readjusted to 7.7, and the solution was mixed on an orbital shaker for 4 h at room temperature. After washing the beads several times with 3 M guanidine hydrochloride in 0.1 M sodium phosphate, pH 8.0, the apo Δ(187−243)A-I+his mutant was eluted from the column using a continuous pH gradient from 3 M guanidine hydrochloride in 0.1 M sodium phosphate, pH 6.3, to 3 M guanidine hydrochloride in 0.1 M sodium phosphate, pH 4.1. Fractions containing apo Δ(187−243)A-I+his were dialyzed against TBS (0.02 M Tris-base, 0.15 M NaCl, 1 mM EDTA, pH 7.4). An extinction coefficient of 1.32 mL/(mg·cm) at 280 nm in 6 M guanidine hydrochloride for apo Δ(187−243)A-I+his was used to determine protein concentration. Factor Xa (New England Biolabs, Beverly, MA) was used to cleave the amino-terminal histidine tag. After cleavage, solid guanidine hydrochloride was added to the protein solution to a final concentration of 3 M, the pH was adjusted to 7.7, and the mixture was added to washed Ni-NTA beads. After a 4 h incubation, the supernatant was collected and analyzed for the presence of the mutant protein using SDS−PAGE, immunoblots, and analytical HPLC. In our hands, the protein was greater than 95% pure using these methods, and was stored lyophilized at −20 °C in the same manner as described for apo hA-I.

Apo Δ(1−43)A-I was purified and characterized as described previously (Rogers et al., 1997) with some modifications. After harvesting, the bacterial cells containing

the mutant protein, apo Δ(1−43)A-I, were lysed by French Press. The pellet was resuspended in 8 M guanidine hydrochloride, and the insoluble material was removed by centrifugation. Acetonitrile was added to the remaining supernatant to a final concentration of 30%, and any precipitate was removed by further centrifugation. The mutant protein, apo Δ(1−43)A-I, was purified from the resulting clear supernatant on a preparative reversed phase HPLC column. HPLC fractions were analyzed by SDS−PAGE, immunoblots, and analytical HPLC. By these methods, the protein was greater than 95% pure, and stored lyophilized at −20 °C.

Boundary Sedimentation Velocity Ultracentrifugation of Apo hA-I, Apo Δ(1−43)A-I, and Apo Δ(187−243)A-I. Boundary sedimentation velocity experiments were performed as described elsewhere (Lebowitz et al., 1994) on a Beckman Model XL-A analytical ultracentrifuge equipped with photoelectric scanners. Boundary sedimentation was performed using a AN60 Ti rotor at 58 000 rpm at 4 and 20 °C in either a low ionic strength buffer (60 mM ammonium bicarbonate) or a high ionic strength buffer (TBS: 20 mM Tris, 150 mM sodium chloride, 1 mM EDTA, pH 7.5). Digital acquisition of the absorbance at 214 nm of the moving boundary was made at regular time intervals.

The net sedimentation behavior of macromolecules in a centrifugal field, *s*, is described by the Svedberg equation:

$$s = \upsilon/\omega^2 r = M(1 - \bar{\upsilon}_2\rho)/Nf \quad (1)$$

where υ is the velocity of the macromolecule along the radial axis ($\Delta r/\Delta t$), ω is the angular velocity of the rotor [2π(rpm)/60], r is the radial distance from the center of rotation, M is the molecular mass, N is Avogadro's number, f is the frictional coefficient related to the molecular size and shape, ρ is the density of the solvent, and $\bar{\upsilon}_2$ is the partial specific volume of the particle.

The frictional ratio of the experimental f value divided by the frictional coefficient of either an unhydrated (f_{min}) or a hydrated sphere (f_o) of identical molecular weight can be calculated from the equations:

$$f/f_{min} = M(1 - \upsilon\rho)/Ns_{w,20}6\pi\eta[(3M\bar{\upsilon}_2)/(4\pi N)]^{1/3} \quad (2)$$

$$f/f_{min} = f/f_o[(\bar{\upsilon}_2 + \bar{\upsilon}_1\Gamma')/\bar{\upsilon}_2]^{1/3} \quad (3)$$

where f/f_{min} is the frictional coefficient ratio due to the shape of the molecule if water is excluded (maximum asymmetry) and f/f_o is the frictional coefficient ratio due to the shape if water is included, M represents the molecular mass of the protein, $\bar{\upsilon}_2$ is the calculated partial specific volume of the unhydrated protein (Table 1), N is Avogadro's number, η is the viscosity of the solution, ρ is the density of the solvent, $\bar{\upsilon}_1$ is the partial specific volume of water, and Γ' is the amount of hydration in grams of H_2O per gram of protein. Γ' was estimated to be 0.35 (Aggerbeck et al., 1988; Barbeau et al., 1979; Laue et al., 1992). From the calculated values of f/f_o, the maximum asymmetry can be determined for prolate or oblate ellipsoids of revolution (Cantor & Schimmel, 1980) using the equation:

$$F = f/f_o = (1 - p^2)^{1/2}/p^{2/3} \ln\{[1 + (1 - p^2)^{1/2}]/p\} \quad (4)$$

for a prolate ellipsoid, where $p = b/a = 1/p_r$; p_r is the axial ratio and F is a shape factor (Perrin factor). This asymmetry may be expressed as the axial ratio (a/b) of the ellipsoid, where a is the radius along the long geometric axis of revolution and b is the short equatorial radius (Table 1; Cantor & Schimmel, 1980). By using the following relationship for the volume of an ellipsoid:

$$M(\bar{\upsilon}_2 + \Gamma'\bar{\upsilon}_1) = 4\pi N(a/b)b^3/3 \quad (5)$$

where $\bar{\upsilon}_2$ and $\bar{\upsilon}_1$ are the partial specific volumes of the protein and solvent, respectively, and (a/b) is the axial ratio due to asymmetry of the major (a) and minor radial (b) axes of the ellipse, the dimensions of the apo A-I monomers can be determined.

Sedimentation Velocity Analysis of hA-I. Van Holde and Weischet (1978) introduced a theoretical basis and experimental tests for a graphical method that removes boundary spreading due to diffusion, thus allowing high resolution of sedimenting systems composed of either a mixture of molecular weight components or multiple conformational states of a single macromolecular component [for a review, see Hansen et al. (1994)]. UltraScan data analysis software developed by B. Demeler was used to perform a van Holde−Weischet analysis of the boundary sedimentation velocity data of native and mutant apo hA-I. The first step in this method is to divide each boundary scan into n exact divisions that are evenly spaced between the base line and the plateau. An apparent sedimentation coefficient (s*) is calculated from the radial point of each of the preselected n boundary divisions. The s_n* values (where subscript n designates the selected boundary fraction) are then plotted versus the inverse square root of time of each scan, and a linear least-squares fit of s_n* versus $t^{-0.5}$ is determined. It can be shown that a graph of s* obtained at a fixed radial value at various times versus $t^{-0.5}$ (diffusion is proportional to $t^{-0.5}$) describes a straight line where, through extrapolation to infinite time, $t^{-0.5}$ approaches zero, and a true s* value can be obtained. In this manner, diffusion effects on boundary shape are eliminated. Plots of s_n* as a function of $t^{-0.5}$ will extrapolate to an essentially single $s_{20,w}$ value for a single ideal component; if multiple components or multiple conformations for a single component are present, the plot will show multiple intercepts. In the van Holde−Weischet analyses, only the boundary region from 10 to 90% is used to eliminate noise inherent in the outer regions (e.g., the meniscus and the plateau).

Reversible Equilibrium Unfolding/Refolding by Difference Spectroscopy. Urea-induced unfolding of lipid-free apo hA-I, apo Δ(1−43)A-I, and apo Δ(187−243)A-I was monitored by circular dichroism [AVIV 62DS spectropolarimeter (AVIV, Lakeside, NJ)], fluorescence [Aminco-Bowman Series 2 fluorometer (SLM-Aminco, Rochester, NY)], and ultraviolet absorbance [Cary 3E UV/visible spectrophotometer (Varian Australia Pty. Ltd., Victoria, Australia)] spectroscopies. Urea stock solutions (10 M) made from Ultrapure urea (Gibco BRL, Grand Island, NY) in PBS, pH 7.4, were prepared fresh for each experiment, and the concentration was verified by refractive index measurements (Warren & Gordon, 1966) using an Abbe Refractometer (American Optical Corp., Buffalo, NY). The experimental design and curve-fitting analysis were carried out as described elsewhere

(Rogers et al., 1997).

ANS (1-Anilinonaphthalene-8-sulfonate) Binding Measurements. ANS (Aldrich, Milwaukee, WI) binding experiments were carried out on solutions containing 50 μg/mL protein [1.8 μM for apo hA-I and 2.3 μM for apo Δ(187−243)A-I] and 250 μM ANS. Carbonic anhydrase (M_r 28 000), a typical water-soluble globular protein, was used as a control (35 μg/mL, 1.4 μM). In all cases, ANS was in at least 100-fold excess of the protein (mol/mol). ANS fluorescence spectra were obtained as described elsewhere (Rogers et al., 1997).

Fluorescence Quenching of Apo hA-I, Apo Δ(1−43)A-I, and Apo Δ(187−243)A-I. Fluorescence quenching of apo hA-I, apo Δ(1−43)A-I, and apo Δ(187−243)A-I was carried out using acrylamide (BioRad, Richmond, CA), iodide (Aldrich, Milwaukee, WI), and trichloroethanol (TCE; Acros Organics, Pittsburgh, PA). Iodide was prepared with 0.1 mM NaS_2O_4 to inhibit the formation of iodine. The iodide concentration varied from 0 to 0.22 M in the quenching experiments, and separate quenching experiments using KCl showed that the effect of changing ionic strength was identical for apo hA-I, apo Δ(1−43)A-I, and apo Δ(187−243)A-I, indicating that comparisons of iodide quenching can be analyzed for effects of iodide only.

TCE-saturated buffer solutions used in quenching were prepared by mixing equal volumes of TCE and PBS (0.02 M sodium phosphate, 0.15 M sodium chloride). Only the top layer of this solution was used for quenching experiments. The concentration of TCE was calculated by assuming a solubility of 8.3% (Merck Index). All quenching studies using TCE were carried out as quickly as possible, and the initial reading after addition of quencher was used (Eftink et al., 1977; Roberts & Dunker, 1993).

Data were collected on a Shimadzu RF5000U spectrofluorophotometer connected to a DR-15 computer with an excitation wavelength of 295 nm and emission wavelength of 330 nm. Buffer solutions containing equivalent amounts of quencher were also measured and subtracted from the protein solutions. Data from at least two experiments were averaged, and Stern−Volmer constants were calculated using the equation:

$$F_o/F = 1 + K_{SV}[Q] \quad (6)$$

where F_o is the emission intensity in the absence of quencher, F is the emission intensity in the presence of quencher, [Q] is the quencher concentration, and K_{sv} is the Stern−Volmer quenching constant. In all cases, r^2 values were 0.95 or better. The Stern−Volmer plots exhibit a slight upward curvature in some cases, possibly corresponding to nonzero values for the static quenching component due to the accumulation of quencher molecules in the region surrounding the tryptophan residues (Lakowicz, 1983) or to spectral differences due to the presence of multiple tryptophans (Eftink & Ghiron, 1976). In these cases, the initial slope of the standard Stern−Volmer plot is used to determine the effective dynamic quenching constant, K_{sv}(eff), and these are reasonable approximations (Eftink et al., 1976).

Circular Dichroism Spectroscopy of Apo hA-I and Apo Δ(1−43)A-I. The CD spectra were recorded with an AVIV 62DS spectropolarimeter interfaced to a personal computer and standardized using a solution of 0.1% (w/v) *d*-10-camphorsulfonic acid. The dynode voltage of each sample was also recorded at the same time as the CD spectrum and was used as an internal standardization of the protein concentration which was determined spectroscopically as described above. The CD spectra were measured every 0.5 nm with 0.5 s averaging per point, and a 2-nm bandwidth, thermostated at 20 °C. A 10 mm path-length cell was used to obtain the near-ultraviolet spectra, and a 0.1 mm path-length cuvette was used to obtain the far-ultraviolet spectra. Spectra were signal-averaged by adding at least four scans; then baseline-corrected by subtracting the spectrum for buffer alone. The spectra were normalized to molar residue ellipticity using a mean residue weight of 115.2 Da for apo hA-I, 115.7 Da for apo Δ(1−43)A-I, and 115.5 Da for apo Δ(187−243)A-I.

Limited Proteolysis of Apo hA-I, Apo Δ(1−43)A-I, and Apo Δ(187−243)A-I. Experiments were conducted as reported in Roberts et al. (1997). Briefly, monomeric protein (0.1 mg/mL) was treated with 200:1 (protein:protease, w/w) chymotrypsin (Calbiochem, La Jolla, CA) at 37 °C for time intervals ranging from 1 to 24 h. Proteolysis was stopped with the addition of a 200 molar excess of 3,4-dichloroisocoumarin over the protease. Proteolytic fragments were separated on Tris−tricine gels (Schagger & von Jagow, 1987) and stained with Coomassie Blue. To analyze the N-terminal sequences of the proteolyzed fragments, gels were blotted onto PVDF paper and analyzed by the Glycoprotein Analysis Core Facility at University of Alabama, Birmingham.

RESULTS

Expression, Purification, and Chemical Characterization of Apo Δ(1−43)A-I and Apo Δ(187−243)A-I Expressed in E. coli. Up to 40 mg of apo Δ(1−43)A-I and 60 mg of apo Δ(187−243)A-I per liter of growth media were purified from an *E. coli* cell lysate. The purity of each protein was assessed by several methods including SDS−PAGE, Western blotting, analytical HPLC, amino acid analysis, and amino-terminal sequencing. A representative Coomassie blue-stained gel and immunoblot probed with a polyclonal antibody raised against apo hA-I (Southern Biotechnology Associates, Birmingham, AL) are shown in Figure 1 (panels A and B, respectively). For apo Δ(1−43)A-I, apo Δ(187−243)A-I+his, and apo Δ-(187−243)A-I mutants, a single protein band is observed with an apparent molecular mass of 24 000 Da (Figure 1A, lane 2), 23 000 Da, and 22 000 Da (Figure 1A, lanes 3 and 4), respectively. These molecular masses are in agreement with those predicted from the amino acid compositions (data not shown).

Boundary Sedimentation Velocity. The dimensions of a macromolecule can be obtained through the sedimentation coefficient, determined by analytical ultracentrifugation. At protein concentrations ranging from 0.1 to 0.2 mg/mL, human apo hA-I, apo Δ(1−43)A-I, and apo Δ(187−243)A-I exhibited smooth sedimentation profiles. Furthermore, it is clear from derivative plots (dc/dt) of the analytical ultracentifugation data [$g^*(s)$ profiles; data not shown] that no significant aggregates of the proteins are present in this concentration range. This result was also confirmed by chemical cross-linking (data not shown). Figure 2 shows representative van Holde−Weischet analyses of the boundary sedimentation velocity data, $s_{20,w}$ versus $t^{-0.5}$, for apo hA-I,

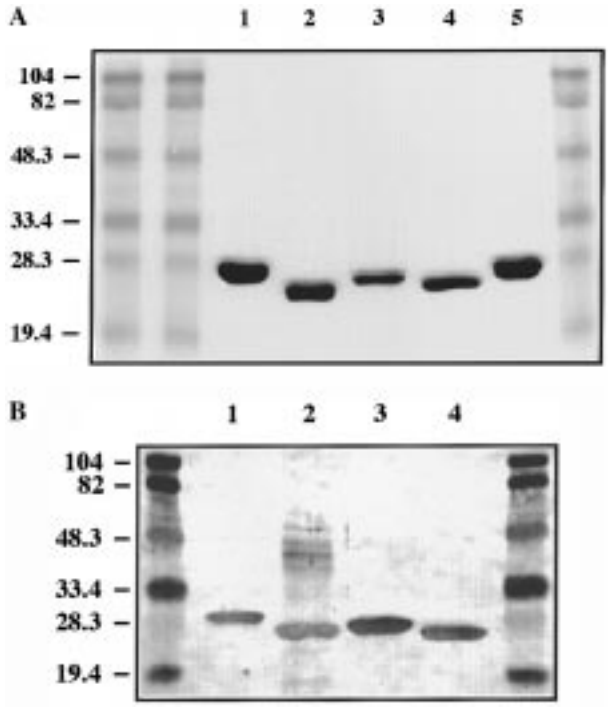

FIGURE 1: (A) SDS−PAGE of purified apo hA-I, apo Δ(1−43)A-I, and apo Δ(187−243)A-I. Lanes 1 and 5, apo hA-I; lane 2, apo Δ(1−43)A-I; lane 3, apo Δ(187−243)A-I+his (before treatment with Factor Xa enzyme); lane 4, apo Δ(187−243)A-I (after treatment with factor Xa enzyme); unlabeled lanes, molecular mass standards; molecular masses in kilodaltons are indicated. (B) Western blot analysis of apo hA-I, apo Δ(1−43)A-I, and apo Δ-(187−243)A-I probed with a polyclonal antibody to apo hA-I. Lane 1, apo hA-I; lane 2, apo Δ(1−43)A-I; lane 3, apo Δ(187−243)A-I+his (before treatment with Factor Xa enzyme); lane 4, apo Δ-(187−243)A-I (after treatment with Factor Xa enzyme); unlabeled lanes, molecular mass standards; molecular masses in kilodaltons are indicated.

apo Δ(1−43)A-I, and apo Δ(187−243)A-I in high ionic strength buffers. The *y*-intercepts correspond to infinite time and yield the diffusion-corrected $s_{20,w}$ at each boundary fraction (Table 1). A sample of macromolecules that is homogeneous with respect to both *M* and *f* yields a single *y*-intercept, while a sample that is heterogeneous with respect to either *M* or *f* yields multiple *y*-intercepts.

Van Holde−Weischet analyses were conducted on each protein at two temperatures (4 and 20 °C) and at two ionic strengths. The different solution conditions were observed to affect predominantly the conformational heterogeneity of each protein, as manifested by the range in $s_{20,w}$ (Hansen et al., 1994), suggesting the proteins exist in several dynamically interchangeable conformations. However, the average $s_{20,w}$ value for each protein remained essentially the same. Therefore, calculated frictional ratios, f/f_{min} and f/f_o, are based on the average from all experiments; at least five experiments per protein were performed (Table 1; see Experimental Procedures for details). Average f/f_o values for apo hA-I and for the mutants were 1.39, 1.35, and 1.35, respectively. The sedimentation coefficients and frictional ratios determined for apo hA-I are in reasonable agreement with values reported previously by Barbeau et al. (1979) and Edelstein and Scanu (1980); however, this analysis has identified a conformational heterogeneity for the monomer where previously only a single monomeric conformer was identified.

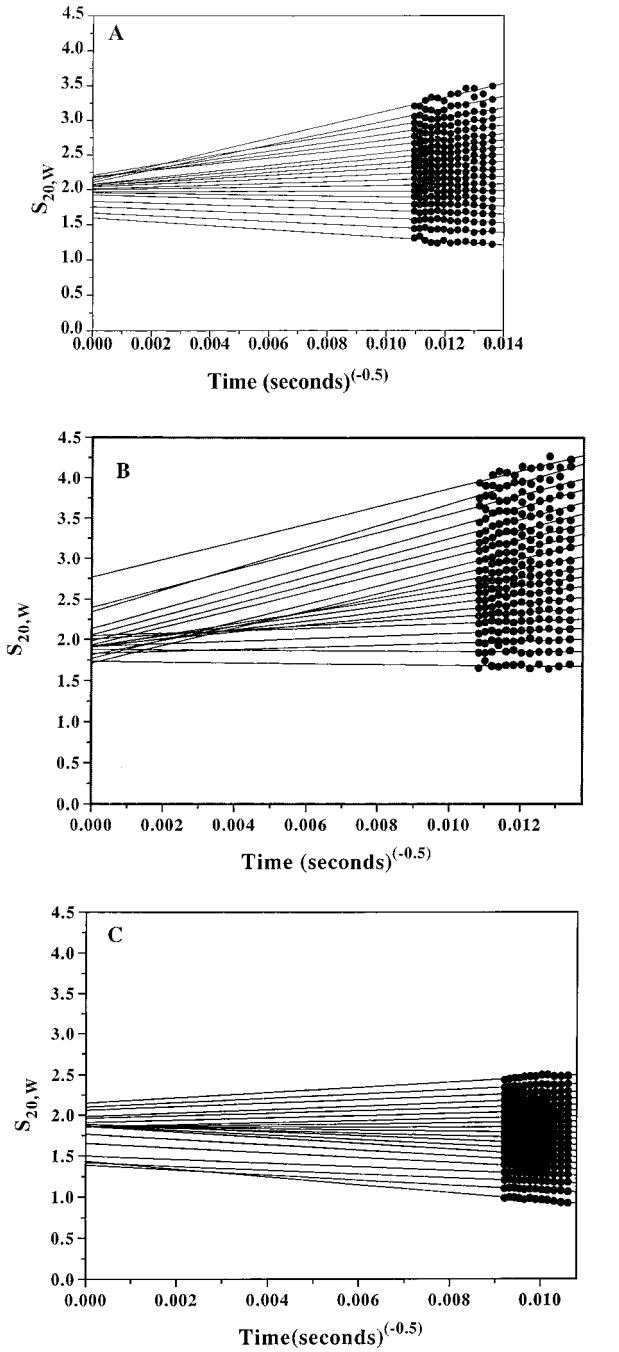

FIGURE 2: Representative van Holde−Weischet extrapolation plots of (A) apo hA-I, (B) apo Δ(1−43)A-I, and (C) apo Δ(187−243)A-I. This analysis of a one-component system indicates multiple *s*-values, ranging from 1.52 to 2.2 S for apo hA-I, from 1.7 to 2.6 S for apo Δ(1−43)A-I, and from 1.45 to 2.1 S for apo Δ(187−243)A-I, which suggests that an equilibrium of monomeric conformers is present at low concentrations (0.1 mg/mL) of the protein (Table 1).

The axial ratios (*a*/*b*) due to asymmetry based on a prolate ellipsoid were estimated to be 7, 6.8, and 6.8 for apo hA-I and the two mutants, apo Δ(1−43)A-I and apo Δ(187−243)A-I, respectively. These ratios indicate that all three apo hA-I monomers are highly asymmetrical (Table 1). The axial ratios translate to an average radial dimension of 8.4 nm by 1.20 nm for the apo hA-I monomer, equivalent to an overall length of 16.8 nm (2*a*). This result is identical to the dimensions cited by Barbeau et al. (1979). The average dimensions calculated for the mutants are very similar to

Table 1: Sedimentation Velocity Properties of Apo hA-I, Apo Δ(1−43)A-I, and Apo Δ(187−243)A-I

apolipoprotein	MW	$\bar{v}_2$[e]	$s_{20,w}$[a] (S)	f/f_{min}	f/f_0	a/b[b]
apo hA-I	28303	0.735	2.05 ± 0.23	1.58 (2.49−1.25)[c] [1.75−1.51][d]	1.39 (2.18−1.10)[c] [1.54−1.32][d]	7.2
apo Δ(187−243)A-I	21601	0.731	1.78 ± 0.25	1.54 (1.96−1.28)[c] [1.90−1.31][d]	1.35 (1.71−1.12)[c] [1.67−1.15][d]	6.8
apo Δ(1−43)A-I	23353	0.738	1.83 ± 0.29	1.54 (2.33−1.06)[c] [1.38−1.08][d]	1.35 (2.04−0.93)[c] [1.21−0.95][d]	6.8

[a] The average $s_{20,w}$ value ± the standard deviation of at least five experiments in which both the ionic strength of the buffer and the temperature varied. [b] The axial ratio calculated (Cantor & Schimmel, 1980) for apo A-I and the mutants based on the f/f_0 assuming a prolate ellipsoid (Barbeau et al., 1979; Edelstein & Scanu, 1980). [c] The range of values calculated for the proteins in a low ionic strength buffer. [d] The range of values calculated for the proteins in a high ionic strength buffer. [e] The partial specific volumes were calculated using the UltraScan data analysis software package according to Cohn et al. (1943).

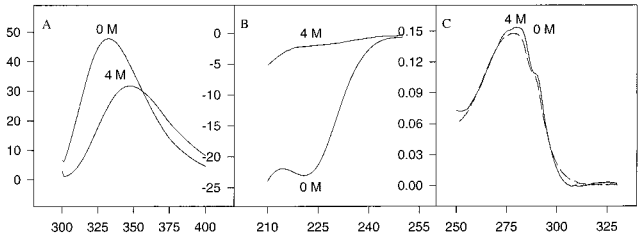

FIGURE 3: (A) Typical fluorescence emission spectra of apo Δ(187−243)A-I in the presence of 4.0 M urea (4 M, completely unfolded state) and in the absence of urea (0 M, native folded state). The *y*-axis is fluorescence intensity, and the *x*-axis is wavelength in nanometers. (B) Typical circular dichroic spectra of apo Δ(187−243)A-I in the presence of 4.0 M urea (4 M) and in the absence of urea (0 M). The *y*-axis is molar ellipticity (deg × cm^2 × $dmol^{-1}$ × 10^3), and the *x*-axis is wavelength in nanometers. (C) Typical absorption spectra of apo Δ(187−243)A-I in the presence of 4.0 M urea (4 M, dashed line) and in the absence of urea (0 M, solid line). The *y*-axis is in absorbance units, and the *x*-axis is wavelength in nanometers.

those calculated for the apo hA-I monomer: $a = 7.8$ and 7.5 nm and $b = 1.14$ and 1.11 nm for apo Δ(1−43)A-I and apo Δ(187−243)A-I, respectively, giving overall lengths of 15.6 and 15 nm ($2a$), respectively.

Measurements of Reversible Equilibrium Unfolding by Spectroscopy. Denaturation of apo hA-I, apo Δ(1−43)A-I (Rogers et al., 1997), and apo Δ(187−243)A-I with urea was monitored using mean residue ellipticity, $[\Theta]_{222}$, difference molar absorptivity, $\Delta\epsilon_m$, and fluorescence emission difference spectroscopy. Figure 3 illustrates typical fluorescence emission, circular dichroic, and absorbance spectra for apo Δ(187−243)A-I in the presence and absence of urea. Similar spectra representative of apo hA-I and apo Δ(1−43)A-I have been illustrated elsewhere (Rogers et al., 1997). The unfolded protein exhibits a lower fluorescence intensity with a concomitant red shift of the peak wavelength, indicating an increase in the polarity of the environment surrounding the tryptophans in response to increased exposure to solvent (Figure 3A). This increase in polarity directly corresponds to the loss of defined secondary structure in the denatured protein as determined by CD (Figure 3B). The absorbance spectra of denatured apo Δ(187−243)A-I indicate a slight decrease in intensity with a slight blue shift of the peak wavelength compared to the native protein (Figure 3C). These results directly reflect the trends seen for both apo hA-I and apo Δ(1−43)A-I (Rogers et al., 1997).

Using a two-state model, a simultaneous global fit of the combined data sets for apo Δ(187−243)A-I (see Figure 4 legend) yielded the parameters ΔG_{H2O}, m_D, and $[\text{urea}]_{1/2}$ (Figure 4 and Table 2). Table 2 gives the ΔG_{H2O}, m_D, and $[\text{urea}]_{1/2}$ values for apo hA-I and apo Δ(1−43)A-I for comparison (Rogers et al., 1997). The data from the urea-induced unfolding of apo hA-I versus apo Δ(187−243)A-I suggest that the C-terminus does not play a major role in the stability of the protein, with ΔG_{H2O} values of 7.41 ± 0.55 kcal/mol for apo Δ(187−243)A-I compared to 9.3 ± 0.55 kcal/mol for apo hA-I (a Student's *t*-test shows that these values are not statistically different, $p > 0.05$; graphically depicted in Figure 5). This is in direct contrast with the amino-terminal deletion mutant, apo Δ(1−43)A-I, which has a more pronounced effect on the stability of the protein, $\Delta G_{H2O} = 4.49 \pm 0.24$ kcal/mol (Rogers et al., 1997).

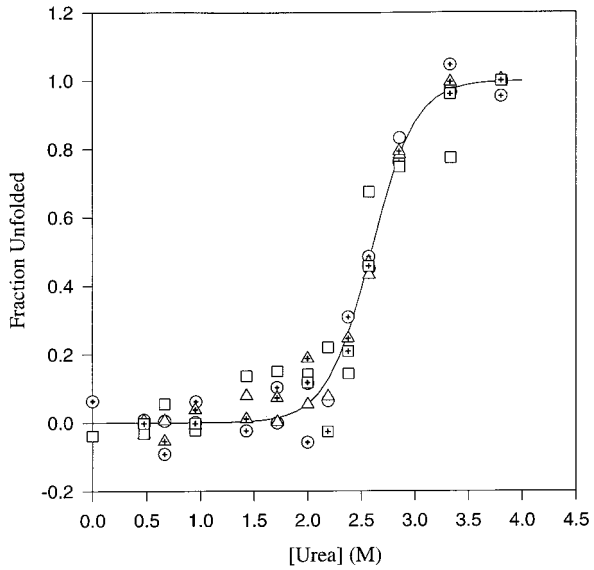

FIGURE 4: Urea-induced unfolding of apo Δ(187−243)A-I monitored using three types of spectroscopic measurements: fluorescence emission, absorbance, and circular dichroism. In order to combine the various difference spectral measurements on a single scale for a global fitting, the experimental data were normalized to the apparent fraction of unfolded protein, f_u, as a function of urea concentration. Symbols represent unfolding and refolding experiments monitored by absorbance (open circle, open hexagon, and open circle with dot, and open square with plus sign are unfolding and refolding, respectively); fluorescence (open triangle with plus sign and triangle are unfolding and refolding, respectively); and circular dichroism (open circle with plus sign is unfolding only). The solid line represents the global two-state fit where multiple sets of data for each protein are combined to determine a single set of thermodynamic parameters (Table 2).

Table 2: Thermodynamic Parameters Associated with Apo hA-I, Apo Δ(1−43)A-I, and Apo Δ(187−243)A-I

apolipoprotein	ΔG_{H2O} (kcal/mol)	m_D (kcal mol^{-1} M^{-1})	$[urea]_{1/2}$ (M)	λ_{max}[a] (nm)
apo hA-I	9.37 ± 0.56[b]	3.55 ± 0.34[b]	2.64	469
apo Δ(187−243)A-I	7.41 ± 0.55[b]	2.85 ± 0.22[b]	2.6	475
apo Δ(1−43)A-I[c]	4.49 ± 0.24	2.41 ± 0.12	1.9	464

[a] ANS binding peak wavelength. [b] A Student's *t*-test indicates there is no statistical significance ($p > 0.05$) between the numbers obtained for apo hA-I and apo Δ(187−243) A-I. [c] Included for purposes of comparison (Rogers et al., 1997).

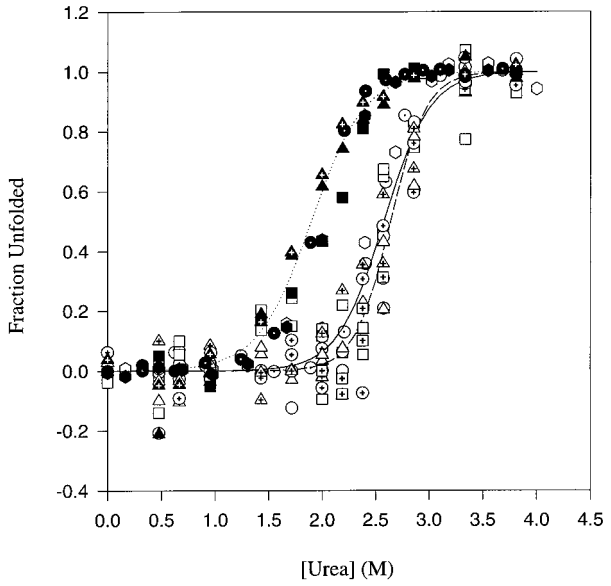

FIGURE 5: Comparison of the urea-induced unfolding profiles of apo hA-I (dashed line), apo Δ(187−243)A-I (solid line), and apo Δ(1−43)A-I (dotted line) monitored using three types of spectroscopic measurements: fluorescence emission, absorbance, and circular dichroism (Rogers et al., 1997). Symbols represent unfolding and refolding experiments as described in Figure 4. The lines represent the global two-state fits where multiple sets of data have been combined to determine a single set of thermodynamic parameters (Table 2).

ANS Binding. The apolar fluorescent dye ANS binds to apo hA-I, apo Δ(1−43)A-I, and apo Δ(187−243)A-I, with an enhanced fluorescence and a blue shift in the wavelength of peak emission (λ_{max}) (Figure 6 and Table 2). ANS in aqueous solutions has a very low quantum yield, 0.004, with an emission maximum at 515 nm (Goto & Fink, 1989). After binding to apo hA-I and apo Δ(187−243)A-I, there is a 70-fold and 40-fold (respectively) increase in fluorescence intensity (with concomitant blue shifts from 515 to 469 and 475 nm, respectively), indicating fewer ANS molecules bind to apo Δ(187−243)A-I than to apo hA-I. As reported earlier (Rogers et al., 1997), there is a substantial increase in fluorescence intensity (approximately 200-fold) when ANS binds to apo Δ(1−43)A-I, with an accompanying blue shift from 515 to 464 nm. These significant increases in relative quantum yields over that for ANS in buffer alone indicate that this compound is binding to an accessible hydrophobic surface or cavity (Stryer, 1965). In direct contrast, no change in fluorescence is associated with ANS binding to carbonic anhydrase (λ_{max} at 515 nm), a stably folded globular protein of similar size that was used as a control (Semisotnov et al., 1987).

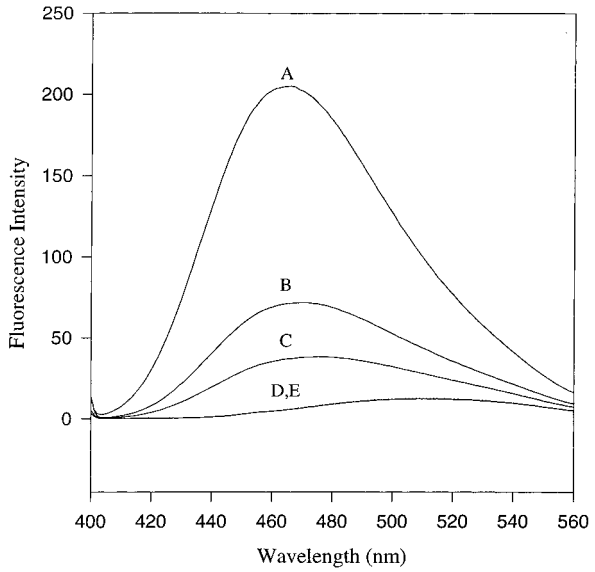

FIGURE 6: ANS binding to (A) apo Δ(1−43)A-I, (B) apo hA-I, (C) apo Δ(187−243)A-I, (D) carbonic anhydrase, and (E) ANS in buffer alone monitored by fluorescence emission.

Fluorescence Quenching. Fluorescent quenchers that interact with proteins can provide information concerning the microenvironment surrounding the tryptophan residue(s). Fluorescence quenching of the three apo A-I variants was carried out using charged (iodide), polar (acrylamide), and nonpolar (TCE) quenchers. Ionic quenchers, because of their charge and significant hydration, are typically able to quench only surface tryptophanyl residues (Eftink & Ghiron, 1976; Lehrer, 1971). Alternatively, acrylamide has been shown to quench the fluorescence of indole derivatives, regardless of where the residue(s) is (are) located (surface or interior) (Eftink & Ghiron, 1976). TCE, a hydrophobic compound, preferentially partitions to the interior of proteins or hydrophobic pockets and can thereby help selectively identify tryptophanyl residues in a hydrophobic microenvironment (Eftink et al., 1976).

The Stern-Volmer (K_{SV}) constants (eq 6), for all of the quenching studies are given in Table 3 (Figure 7). The dynamic quenching constants for acrylamide, iodide, and TCE show essentially no change between apo hA-I and apo Δ(187−243)A-I (each have the same number of tryptophan residues). While apo Δ(1−43)A-I is quenched with iodide to the same degree as apo hA-I and apo Δ(187−243)A-I, this N-terminal deletion mutant exhibits modest differences in quenching by acrylamide and a dramatically different quenching behavior by TCE.

It is interesting to note that a slight curvature is also seen in the Stern−Volmer plots for apo hA-I and apo Δ(187−243)A-I in TCE (0.14 M). This may indicate that, like apo Δ(1−43)A-I, these proteins undergo a TCE-induced conformational change (Eftink et al., 1976; Roberts & Dunker, 1993) but at much higher concentrations of TCE than that seen for apo Δ(1−43)A-I. The concentration dependence of the TCE-induced spectral changes is consistent with the lower stability (ΔG_{H2O}) of apo Δ(1−43)A-I compared to apo hA-I and apo Δ(187−243)A-I.

Near-Ultraviolet Circular Dichroism. Near-UV circular dichroic spectra (250−330 nm) show a series of positive and negative extrema which reflect the combined contribution

Table 3: Analysis of Lipid-Free Apo hA-I, Apo Δ(1−43)A-I, and Apo Δ(187−243)A-I

	K_{SV}[a]				
apolipoprotein	iodide	acrylamide	TCE	% α-helix	helical aa[c]
apo hA-I	3.9 ± 0.6	6.5 ± 0.1	12.5 ± 1.0	68 ± 4	165
apo Δ(1−43)A-I	3.8 ± 0.1	8.3 ± 0.2	51.8 ± 2.01	82 ± 2	165
apo Δ(187−243)A-I	3.8[b]	6.5 ± 0.0	14.1 ± 0.8	68 ± 5	127

[a] Stern−Volmer constants, determined using eq 5, represent the average ± SD of three trials except where indicated. [b] This Stern−Volmer constant represents one trial. [c] The number of helical amino acids (aa) in the protein is estimated by multiplying the fractional helicity by the number of residues in the protein [apo hA-I = 243; apo Δ(1−43)A-I = 201; apo Δ(187−243) A-I = 186].

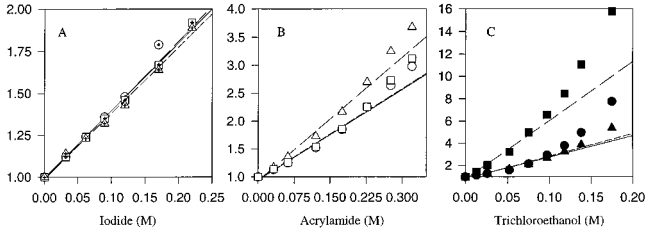

FIGURE 7: Stern−Volmer plots of (A) iodide-, (B) acrylamide-, and (C) trichloroethanol-based fluorescence quenching from intensity measurements of lipid-free apo hA-I (circle, solid lines), apo Δ(1−43)A-I (square, long dashed lines), and apo Δ(187−243)A-I (triangle, short dashed lines). The Stern−Volmer constants were obtained from eq 6 using the linear portion of the graph (Table 3).

of all the aromatic amino acid residues; tryptophan, tyrosine, and phenylalanine; only proteins with a folded tertiary structure exhibit such a profile. Apo hA-I contains four tryptophans, seven tyrosines, and five phenylalanines. In deleting the first 43 residues, tryptophan 8, tyrosines 18 and 29, and phenylalanine 33 have been eliminated. In removing the last 57 residues, tyrosines 192 and 236 and phenylalanines 225 and 229 were deleted. The overall spectra for apo hA-I and apo Δ(187−243)A-I are remarkably similar in both the shape and the intensity of the peaks. The major difference between these spectra occurs in the phenylalanine vibronic region (250−265 nm) (Strickland, 1974) which can be attributed to the deletion of two phenylalanines from apo Δ(187−243)A-I. Interestingly, this deletion did not change the tyrosine vibronic region between 284 and 273 nm, and only affected the intensity of the phenylalanine peak found between 265 and 250 nm, indicating only changes in the side chain mobility of the aromatic residues and those residues in their immediate vicinity (Strickland, 1974). In contrast, the spectra of apo hA-I and apo Δ(1−43)A-I (Figure 8, included for comparison) are very different, including a blue shift of the tryptophan signature wherein the vibronic band shifts to 295 nm in apo Δ(1−43)A-I (Rogers et al., 1997).

Far-Ultraviolet Circular Dichroism. Far-UV CD was used to compare the relative secondary structure content of lipid-free apo hA-I, apo Δ(187−243)A-I, and apo Δ(1−43)A-I (Rogers et al., 1997). The average percent α-helical content of apo hA-I and apo Δ(187−243)A-I, obtained from multiple preparations, is roughly the same, yet apo hA-I contains more residues per molecule in an α-helix (Table 3). On the other hand, lipid-free apo Δ(1−43)A-I contains the same number of residues in an α-helix as lipid-free apo hA-I, suggesting that the carboxy terminus has become more helical relative to lipid-free apo hA-I (Rogers et al., 1997). This result has important consequences for lipid binding which will be discussed later.

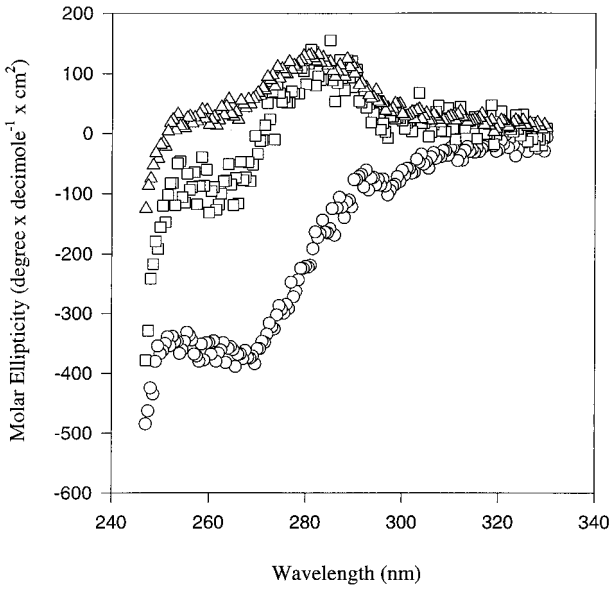

FIGURE 8: Near-UV CD of apo hA-I (square), apo Δ(1−43)A-I (circle), and apo Δ(187−243)A-I (triangle) to detect differences in the asymmetric environments surrounding aromatic residues.

Limited Proteolysis of Lipid-Free Apo A-I, Apo Δ(1−43)A-I, and Apo Δ(187−243)A-I Using Chymotrypsin. Limited proteolysis is a valuable tool for probing the tertiary structures of proteins, specifically apo A-I, and has been used by a number of investigators to study apo A-I conformations [reviewed in Brouillette and Anatharamaiah (1995), Dalton and Swaney (1993), Ji and Jonas (1995), Lins et al. (1993), and Roberts et al. (1997)]. We have done an extensive analysis of the domain structure of lipid-free and lipid-bound apo hA-I using chymotrypsin and *S. aureus* V_8 as probes (Roberts et al., 1997). These studies enabled a comparison study of lipid-free apo hA-I, apo Δ(1−43)A-I, and apo Δ(187−243)A-I to be performed using chymotrypsin, which cleaves on the carboxy-terminal side of accessible aromatic and bulky, hydrophobic amino acids.

Treatment of monomeric, lipid-free apo hA-I with chymotrypsin results in the appearance of one major product by PAGE (see Experimental Procedures) after 1 h of cleavage. This product has a native N-terminus with a molecular mass (22.4 kDa, Table 4) that is consistent with cleavage at Y_{192} as previously observed (Ji & Jonas, 1995; Roberts et al., 1997). Several minor bands become apparent between 1 and 4 h of cleavage (data not shown; Roberts et al., 1997). Sequence analysis of these products is summarized in Table 4. The observed cleavage sites are consistent with other data for apo hA-I (Roberts et al., 1997) with the exception of a minor product from cleavage at F_{57}, which most likely can be attributed to the presence of 10-

Table 4: Limited Proteolysis of Apo A-I Variants Using Chymotrypsin

	apo hA-I			apo Δ(1−43)A-I			apoΔ(187−243)A-I		
Tris−tricine band	molecular mass[a]	N-term. sequence[b]	cleavage[c]	molecular mass[a]	N-term. sequence[b]	cleavage[c]	molecular mass[a]	N-term. sequence[b]	cleavage[c]
native	28.3	DEPPQ	none	23.6	MLKLL	none	21.6	DEPPQ	none
major	22.4	DEPPQ	D_1-Y_{192}	17	RAELQ	$L_{122}-Q_{243}$	21.6	DEPPQ	D_1-G_{186}
major				15	SKLRE	$F_{57}-L_{181}$			
major				15	RAELQ	$L_{122}-Y_{236}$			
minor[d]	15.7	SKLRE	$F_{57}-Y_{192}$	18.4	SKLRE	$F_{57}-Q_{243}$			
minor[d]	14.2	RAELQ	$L_{122}-Q_{243}$						
minor[d]	14.2	DEPPQ	D_1-L_{122}						

[a] Molecular mass is expressed in kilodaltons. [b] Amino-terminal sequence of the resultant peptides (see Experimental Procedures for details). [c] Represents the resultant peptide fragment after cleavage. [d] These fragments represent less than 10% of the final products observed.

fold more enzyme in this proteolysis experiment compared to that reported earlier.

Treatment of monomeric apo Δ(187−243)A-I with chymotrypsin resulted in no discernible cleavage at 1 h, since the only protein visible by PAGE was intact apo Δ(187−243)A-I based on migration and its N-terminal sequence, D_1-EPPQ (Table 4). The small discrepancy in size between this fragment and the equivalent fragment seen in proteolyzed apo hA-I (D_1-Y_{192}) can be accounted for by six residues, $A_{187}RLAEY_{192}$, which are missing from the C-terminus of apo Δ(187−243)A-I. The minor cleavage sites observed in apo hA-I were not present in apo Δ(187−243)A-I until the 4 h time point (data not shown).

While chymotrypsin cleaved both apo hA-I and apo Δ(187−243)A-I in a similar manner, different proteolytic fragments were obtained from apo Δ(1−43)A-I. Limited proteolysis of apo Δ(1−43)A-I results in three major peptides after 1 h of chymotryptic cleavage, none of which contained the native N-terminus ($ML_{44}KLL$). These peptides presented the N-terminal sequences $R_{123}AELQ$ (17 kDa), $S_{58}KLRE$ (15 kDa), and $R_{123}AELQ$ (15 kDa), which correspond to cleavage at F_{57}, L_{122}, L_{181}, and Y_{236} (Table 4). The pattern of susceptibility of these sites in apo Δ(1−43)A-I to cleavage is strikingly similar to the pattern seen for chymotrypsin cleavage of lipid-bound apo hA-I (Roberts et al., 1997) rather than lipid-free apo hA-I.

DISCUSSION

Previous studies employing limited proteolysis of apo hA-I revealed major cleavage sites in the C-terminus of the lipid-free protein, particularly near residue 192 (Ji & Jonas, 1995; Roberts et al., 1997), and in the N-terminus of the lipid-bound protein, particularly near residue 43 (Roberts et al., 1997). We have developed a bacterial expression system for apo hA-I (Rogers et al., 1997) to enable structural studies on the products derived from these two cleavages, with the belief that the deletion mutants would hold clues about apo hA-I's two conformational states and the transition between them (Roberts et al., 1997; Rogers et al., 1997). Previously we showed by a wide variety of spectroscopic and other physical measurements that lipid-free apo Δ(1−43)A-I has a conformation more similar to the lipid-bound conformation of apo hA-I (Rogers et al., 1997). Further support for this observation is provided here by the similar proteolytic cleavage patterns exhibited by lipid-free apo Δ(1−43)A-I and lipid-bound apo hA-I. Additionally, the marked difference in the fluorescence quenching by the hydrophobic solvent TCE is consistent with a fundamentally different fold for the two lipid-free proteins. We conclude that deletion of residues 1−43 produces a new conformation because the missing residues are an integral part of the native fold of lipid-free apo hA-I. In the present studies, we also show the lipid-free structure of apo Δ(187−243)A-I is similar to lipid-free apo hA-I, consistent with our predictions from limited proteolysis (Roberts et al., 1997). Even though 57 residues have been lost, the structural stability, near-UV CD, and proteolysis patterns are very similar for the two proteins, as are the binding of three fluorescence quenchers with very different polarities. These data are most consistent with a folded structure that is largely unchanged by the absence of the carboxy terminus. The slightly lower helicity and lower ANS binding of apo Δ(187−243)A-I suggest some loss of structure in the carboxy terminus due to the nature of the deletion, however.

The analytical ultracentrifugation results have given a unique insight into the conformational dynamics of these proteins that should bear on their lipid binding properties. Sedimentation velocity experiments indicate that apo hA-I and the deletion mutants, apo Δ(1−43)A-I and apo Δ(187−243)A-I, exist as an equilibrium of conformers in the lipid-free state. At low concentrations (0.1 and 0.2 mg/mL), 80% of each protein exists as a highly elongated molecule with average dimensions of approximately 15.0−16.8 nm by 2.2−2.4 nm [similar dimensions were reported for apo hA-I by Barbeau et al. (1979)]. Another 10% of the monomers correspond to a more compact protein with dimensions of 10 nm × 2.8 nm. A small percentage (∼10%) of the molecules in the population exhibit axial ratios of 12 or 14, most likely representing end-on-end aggregates of the elongated conformer; such molecules exhibit very small $s_{20,w}$ values (<1.6; see Figure 2). It is interesting that the deletion of either the amino or the carboxy terminus had relatively minor effects on the sedimentation velocity results. This suggests that the modular nature of the amphipathic helix allows for some shape adaptation to occur in the elongated conformation. A hypothetical model for the more compact conformer of apo hA-I was proposed earlier (Figure 9A, Roberts et al., 1997); the present results suggest it is in equilibrium with an elongated conformer that unfolds in a hingelike manner to yield the structure shown in Figure 9B. (A third state representing end-on-end aggregates of the elongated conformer is not shown.)

Consistent with the observed dynamic equilibrium described by analytical ultracentrifugation, apo hA-I and its variants have accessible or exposed hydrophobic surface(s) or pocket(s) to the hydrophobic probe ANS (Stryer, 1965).

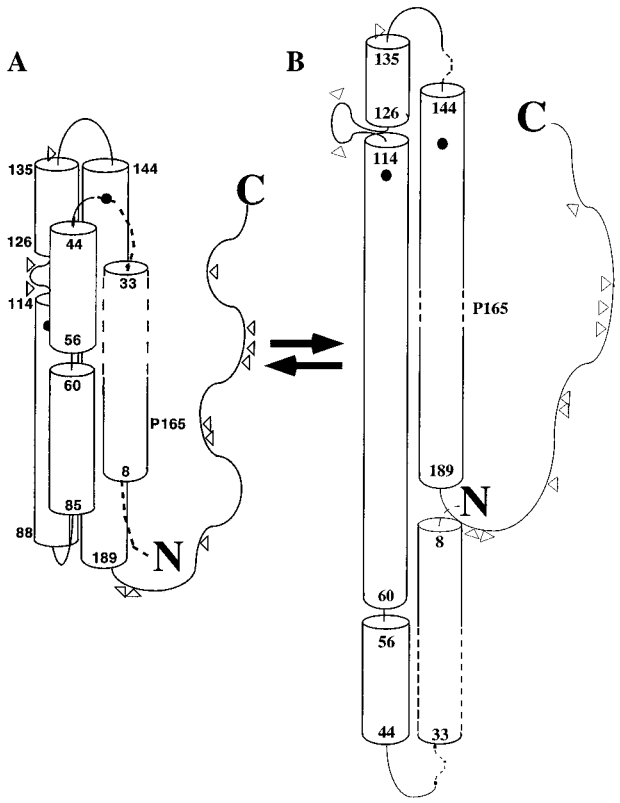

FIGURE 9: Proposed conformational equilibrium for lipid-free apo hA-I. (A) Folded four-helix bundle conformation, as adapted from Roberts et al. (1997). (B) Elongated, monomeric helical hairpin derived from analytical ultracentrifugation. Cylinders represent helical structures. The filled circles represent the positions of methionines 112 and 148. Arrowheads indicate positions of cleavage sites in the reduced protein, adapted from Roberts et al. (1997). Dashed lines depict regions of probable secondary structure, which may or may not represent helical amino acids.

The increase in fluorescence intensity and the blue-shifts observed for ANS when bound to apo hA-I, apo Δ(1−43)A-I, and apo Δ(187−243)A-I support the existence of a range of discrete, interchangeable conformations in which the molecule flexes to allow small hydrophobic molecules into the interior of the protein. Complementary data using TCE and acrylamide as fluorescence quenching reagents provided a similar picture of the structures of the three proteins.

Conclusions. We report here the first direct evidence for the presence of conformational heterogeneity or plasticity in lipid-free apo hA-I which could play a role in lipid binding. The first step in lipid binding is widely thought to occur via binding of the extreme carboxy terminus of apo hA-I[1] (Ji & Jonas, 1995; Gursky & Atkinson, 1996; Roberts et al., 1997; Rogers et al., 1997), probably mediated through some discrete secondary structure present in this predominantly unfolded and uncooperative region. Since apo hA-I must unfold to expose hydrophobic domains for lipid binding (Roberts et al., 1997; Rogers et al., 1997), the elongated conformer observed here may be a lipid binding intermediate, representing the product of a conformational change in apo hA-I that occurs either prior to or after binding of the carboxy terminus. As previously discussed (Rogers et al., 1997), we conclude that later stages in binding require the communication of the initial binding step to the amino-terminus (represented by at least residues 1 through 43) which induces a conformational change in the protein. As a result of this conformational change, additional lipid binding sites (between residues 44−189) are exposed and made available to bind to lipid. Many biophysical studies on apo hA-I have focused attention on its conformation when bound to discoidal reconstituted lipoproteins. The lipid binding model which is emerging from our recent structural studies is consistent with several possibilities for a lipid-bound conformation(s), including a model wherein the amphipathic helical axes are perpendicular to the fatty acyl chains (Borhani et al., 1997). Future studies will more directly address the details of this model.

[1] Even at concentrations where apo hA-I is highly aggregated, the monomeric form is still present, suggesting a dynamic equilibrium exists between monomer and multimers. At concentrations as high as 2.0 mg/mL, the 2.0S component (*i.e.*, monomeric apo hA-I) is still observed (Barbeau et al., 1979; Edelstein & Scanu, 1980). While our research focuses on the monomeric conformation of apo hA-I, even at apo hA-I concentrations where considerable quaternary structure is present, this observation is consistent with a monomer-initiated lipid binding model.

ACKNOWLEDGMENT

We thank Marjorie Ray and Barry Heard for their assistance in purifying the proteins, Susan Tendian for her assistance in the equilibrium unfolding/refolding data analysis, Rodney Ott for his experience with the Model XLA ultracentrifuge, and Dr. Don Muccio for his expertise and assistance in analyzing the circular dichroic spectra.

REFERENCES

Acton, S., Rigotti, A., Landschulz, K. T., Xu, S., Hobbs, H. H., & Krieger, M. (1996) *Science 271*, 518−520.
Aggerbeck, L. P., Wetterau, J. R., Weisgraber, K. H., Wu, C.-S. C., & Lindgren, F. T. (1988) *J. Biol. Chem. 263*, 6249−6258.
Allan, C. M., Fidge, N. H., Morrison, J. R., & Kanellos, J. (1993) *Biochem. J. 290*, 449−455.
Anantharamaiah, G. M., Hughes, T. A., Iqbal, M., Gawish, A., Neame, P. J., Medley, M. F., & Segrest, J. P. (1988) *J. Lipid Res. 29*, 309−318.
Atkinson, D., Smith, H. M., Dickson, J., & Autsin, J. P. (1976) *Eur. J. Biochem. 64*, 541−547.
Atkinson, D., Small, D. M., & Shipley, G. G. (1980) *Ann. N.Y. Acad. Sci. 348*, 284−298.
Barbeau, D. L., Jonas, A., Teng, T., & Scanu, A. M. (1979) *Biochemistry 18*, 362−369.
Borhani, D. W., Rogers, D. P., Engler, J. A., & Brouillette, C. G. (1997) *Proc. Natl. Acad. Sci. U.S.A. 94*, 12291−12296.
Brasseur, R. (1991) *J. Biol. Chem. 266*, 16120−16127.
Brasseur, R., De Meutter, J., Vanloo, B., Goormaghtigh, E., Ruysschaert, J. M., & Rosseneu, M. (1990) *Biochim. Biophys. Acta 1043*, 245−252.
Briter, D. R., Kanost, M. R., Benning, M. M., Wesenberg, G., Law, J. H., Wells, M. A., Rayment, I., & Holden, H. M. (1991) *Biochemistry 30*, 603−608.
Brouillette, C. G., & Anantharamaiah, G. M. (1995) *Biochim. Biophys. Acta 1256*, 103−129.
Brown, E. M., Kumosinski, T. F., & Farrell, H. M., Jr. (1994) *ACS Symp. Ser. 576*, 100−112.
Cheung, P., & Chan, L. (1983) *Nucleic Acids Res. 11*, 3703−3715.
Cohn, E. J., & Edsall, J. T. (1943) in *Proteins, Amino Acids and Peptides as Ions and Dipolar Ions*, pp 370−381, Reinhold, New York.
Dalton, M. B., & Swaney, J. B. (1993) *J. Biol. Chem. 268*, 19274−19283.
Edelstein, C., & Scanu, A. M. (1980) *J. Biol. Chem. 255*, 5747−5754.
Eftink, M. R., & Ghiron, C. (1976a) *Biochemistry 15*, 672−680.
Eftink, M. R., & Ghiron, C. (1976b) *J. Phys. Chem. 80*, 486−493.

Eftink, M. R., Zajicek, J. L., & Ghiron, C. (1977) *Biochim. Biophys. Acta 491*, 473−481.
Fielding, C. J., & Fielding, P. E. (1995) *J. Lipid Res. 36*, 211−228.
Fielding, C. J., Shore, V. G., & Fielding, P. E. (1972) *Biochem. Biophys. Res. Commun. 46*, 1493−1498.
Fontana, A., Fassina, G., Vita, C., Dalzoppo, D., Zamai, M., & Zambonin, M. (1986) *Biochemistry 25*, 1847−1851.
Forte, T. M., Nichols, A. V., Gong, E. L., Lux, S., & Levy, R. I. (1971) *Biochim. Biophys. Acta 248*, 381−386.
Glomset, J. A. (1968) *J. Lipid Res. 9*, 155−167.
Goto, Y., & Fink, A. L. (1989) *Biochemistry 28*, 945−952.
Gursky, O., & Atkinson, D. (1996) *Proc. Natl. Acad. Sci. U.S.A. 93*, 2991−2995.
Hansen, J. C., Lebowitz, J., & Demeler, B. (1994) *Biochemistry 33*, 13155−13163.
Haynie, D. T., & Freire, E. (1993) *Proteins: Struct., Funct., Genet. 16*, 115−140.
Hughes, T. A., Moore, M. A., Neame, P., Medley, M. F., & Chung, B. H. (1988) *J. Lipid Res. 29*, 363−376.
Ji, Y., & Jonas, A. (1995) *J. Biol. Chem. 270*, 11290−11297.
Lakowicz, J. R. (1983) *Principles of Fluorescence Spectroscopy*, pp 258−281, Plenum Press, New York.
Laue, T. M., Shah, B. D., Ridgeway, T. M., & Pelletier, S. L. (1992) *Analytical Ultracentrifugation in Biochemistry and Polymer Science*, pp 90−125, Royal Society of Chemistry, Cambridge, U.K.
Lebowitz, J., Kar, S., Braswell, E., McPherson, S., & Richard, D. L. (1994) *Protein Sci. 3*, 1374−1382.
Lehrer, S. S. (1971) *Biophys J. 11*, 72a.
Lins, L., Piron, S., Conrath, K., Vanloo, B., Brasseur, R., Rosseneu, M., Baert, J., & Ruysschaert, J.-M. (1993) *Biochim. Biophys. Acta 1151*, 137−142.
Nolte, R. T., & Atkinson, D. (1992) *Biophys. J. 63*, 1221−1239.
Oram, J. F. (1986) *Methods Enzymol. 129*, 645−659.
Pownall, H. J., & Massey, J. B. (1986) *Methods Enzymol. 128*, 515−518.
Privalov, J. (1979) *Nature 280*, 693−696.
Reijngoud, D.-J., & Phillips, M. C. (1982) *Biochemistry 21*, 2969−2976.
Roberts, L. M., & Dunker, A. K. (1993) *Biochemistry 32*, 10479−10488.
Roberts, L. M., Ray, M. J., Shih, T., Hayden, E., Reader, M. M., & Brouillette, C. G. (1997) *Biochemistry 36*, 7615−7624.
Rogers, D. P., Brouillette, C. G., Engler, J. A., Tenidan, S. W., Roberts, L., Mishra, V. K., Anantharamaiah, G. M., Lund-Katz, S., Phillips, M. C., & Ray, M. J. (1997) *Biochemistry 36*, 288−300.
Schagger, H., & von Jagow, G. (1987) *Anal. Biochem. 166*, 368−379.
Schmidt, H. H.-J., Remaley, A. T., Stonik, J. A., Ronan, R., Wellmann, A., Thomas, F., Zech, L. A., Brewer, H. B., Jr., & Hoeg, J. M. (1995) *J. Biol. Chem. 270*, 5469−5475.
Schultz, J. R., Verstuyft, J. G., Gong, E. L., Nichols, A. V., & Rubin, E. M. (1993) *Nature 365*, 762−764.
Segrest, J. P., De Loof, H., Dohlman, J. G., Brouillette, C. G., & Anantharamaiah, G. M. (1990) *Proteins: Struct., Funct., Genet. 8*, 103−117.
Segrest, J. P., Jones, M. K., De Loof, H., Brouillette, C. G., Venkatachalapathi, Y. V., & Anantharamaiah, G. M. (1992) *J. Lipid Res. 33*, 141−166.
Semisotnov, G. V., Rodionova, N. A., Kutyshenko, V. P., Ebert, B., Blanck, J., & Ptitsyn, O. B. (1987) *FEBS Lett. 224*, 9−13.
Semisotnov, G. V., Rodionova, N. A., Razgulyaev, O. I., Uversky, V. N., Gripas, A. F., & Gilmanshin, R. I. (1991) *Biopolymers 31*, 119−128.
Strickland, E. H. (1974) *CRC Crit. Rev. Biochem. 2*, 113−175.
Stryer, L. (1965) *J. Mol. Biol. 13*, 482−495.
Studier, F. W., & Moffat, B. A. (1986) *J. Mol. Biol. 189*, 113.
Sviridov, D., Pyle, L., & Fidge, N. (1996) *Biochemistry 35*, 189−196.
Swaney, J. B., & O'Brien, K. J. (1976) *Biochem. Biophys. Res. Commun. 71*, 636−643.
Van Holde & Weischet (1978) *Biopolymers 17*, 1387−1403.
Viera, J., & Messing, J. (1987) *Methods Enzymol. 153*, 3.
Wald, J. H., Goormaghtigh, E., De Meutter, J., Ruysschaert, J.-M., & Jonas, A. (1990) *J. Biol. Chem. 265*, 20044−20050.
Wang, N., Weng, W., Breslow, J. L., & Tall, A. R. (1996) *J. Biol. Chem. 271*, 21001−21004.
Warden, C., Hedrick, C. C., Quao, J.-H., Castellani, L. W., & Lusis, A. J. (1993) *Science 261*, 469−471.
Wilson, C., Wardell, M. R., Weisgraber, K. H., Mahley, R. W., & Agard, D. A. (1991) *Science 252*, 1817−1822.
Zoller, M. J., & Smith, M. (1983) *Methods Enzymol. 100*, 468.

BI9713512